

CsI(Tl) Micro-Pixel Scintillation Array for Ultra-high Resolution Gamma-ray Imaging

M. N. Cinti, R. Scafè, R. Pellegrini, C. Trotta, P. Bennati, S. Ridolfi, Nico Lanconelli, L. Montani, F. Cusanno, F. Garibaldi, J. Telfer, and R. Pani, *Member, IEEE*

Abstract—The aim of this paper is to investigate the intrinsic spatial resolution limit by coupling a CsI(Tl) micro-pixel scintillation array to position sensitive photomultipliers (PSPMTs) for ultra-high resolution gamma-ray imaging. On this purpose, 1 mm thick array with 0.2 mm pixel side, 0.4 mm pitch has been realized by Spectra Physics (Hilger). The present scintillation arrays technology is suitable to produce larger crystal areas. In this paper we present spatial resolution and positioning results obtained by coupling the micro-pixel scintillation array to Hamamatsu square PSPMTs: 1" R8520-C12, 1" R5900-L16 and 2" H8500 Flat panel PMT. Preliminary measurements demonstrate better performance in term of uniformity response when micro-pixel array is coupled to a H8500 PSPMT model. This setup carries out an intrinsic spatial resolution lower limit of about 0.6 mm FWHM at 50% FWHM energy resolution, defining it as the minimum scintillation array pitch detectable at 122 keV. The results obtained by R5900-L16 with a better sampling of the scintillation light has shown an improvement of the position linearity in spite of a worse spatial resolution due to the poor light output of scintillation array.

Index Terms—Biomedical nuclear imaging, photomultipliers, scintillation detectors.

I. INTRODUCTION

THE increasing interest on pinhole collimation of gamma rays for *in vivo* molecular imaging of small animals is triggering the demand of new imagers' development. In fact, pinhole gamma camera imaging offers the ability to obtain high resolution images from a single gamma ray emitting radiotracers and plays a reasonable trade-off between very small FoV and sensitivity. For many applications on small animals it fulfills the requirements of the specific research where only a small anatomic portion like the brain or the hearth need to be analyzed with the best spatial resolution achievable. Triple heads gamma camera equipped with a sub-millimeter pinhole aperture could be a possible but expensive and cluttering solution. Recently, the technological advances have been making available small FoV detectors with very high intrinsic spatial resolution performances, allowing to build compact detection sys-

tems. A small detection area usually requires a lower magnification factor which avoids to small system FoVs. As a consequence, to have a still good total spatial resolution value we would need higher intrinsic spatial resolution to compensate the lower magnification factor. To overcome this problem, Spectra Physics (Hilger) proposed the realization of a CsI(Tl) scintillation array with 0.2 mm pixel size (0.4 mm pitch), which is the smallest pitch available for this scintillator. This crystal array can be produced with 1 mm thick and large area, pushing Nuclear Medicine imaging close to radiological performances. The CsI(Tl) is a promising material to this purpose: in fact it carries out enough scintillation light when assembled in arrays. Furthermore, it is easily machined and its good radiation absorption at 140 keV provides reasonable intrinsic detection efficiency (30%) for 1 mm crystal thickness. Other possible competitors are the YAP(Ce) and the NaI(Tl). The YAP(Ce) array is realized with pixel size of 0.5 mm (the optical isolation is not necessary), but its lower absorption property involves just few millimeter thickness of the array. Although, NaI(Tl) shows the best light output, its pixel size can not be reduced to less than 1 mm because of its intrinsic difficulty in machining.

Over the last seven years the PSPMT performances have been strongly enhanced by metal channel dynodes allowing intrinsic spread of charges of less than 1 mm FWHM during multiplication processes.

The aim of this paper is to investigate the spatial resolution limit by coupling the CsI(Tl) micro-pixel array to the latest generation of Hamamatsu PSPMTs like R8520-C12, R5900-L16 and H8500 Flat Panel PMT.

II. EQUIPMENT AND METHOD

The CsI(Tl) micro-pixel array is shown in Fig. 1 where the size of each individual pixel ($200 \times 200 \mu\text{m}$) is well recognizable. The overall area is composed of 60×60 elements covering $24 \text{ mm} \times 24 \text{ mm}$.

The PSPMT have strongly improved their intrinsic spatial resolution performances, though still limited by the photocathode glass window thickness needed for the mechanical stress resistance. In contrast with the first generation of PSPMTs, tube compactness allows to reduce the glass window thickness and obtain very narrow charge distributions. Applying the light centroid method, the intrinsic spatial resolution, for brute force calculation, is given by the product between the charge spread and the energy resolution. It means that in principle PSPMT can carry out spatial resolution values less than 0.5 mm.

Three Hamamatsu PSPMTs of latest generation with different glass window thickness and different anode configuration and

Manuscript received November 15, 2003; revised March 15, 2006.

M. N. Cinti, R. Pellegrini, C. Trotta, P. Bennati, S. Ridolfi, and R. Pani are with the Department of Experimental Medicine and Pathology, University of Rome La Sapienza, INFN-Roma I, 00166 Rome, Italy (e-mail: marianerina.cinti@uniroma1.it).

R. Scafè and L. Montani are with ENEA TEC, CR-Casaccia, 301-00060 S. Maria di Galeria Rome, Italy.

N. Lanconelli is with the Department of Physics, University of Bologna, 40127 Bologna, Italy.

F. Cusanno and F. Garibaldi are with the Laboratory of Physics, 00166 Rome, Italy.

J. Telfer is with Spectra Physics—Laser and Photonics Hilger Crystals, Margate Kent CT9 4JL, U.K.

Digital Object Identifier 10.1109/TNS.2007.891227

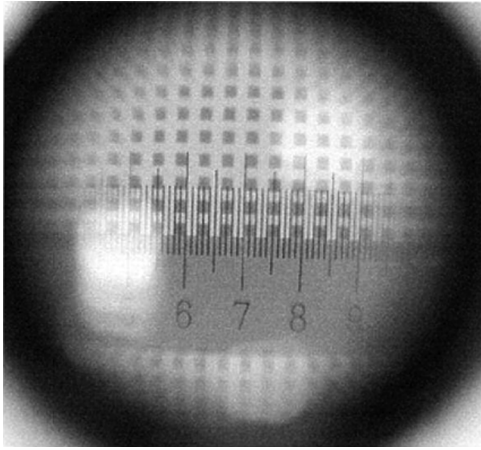


Fig. 1. Picture of the micro-pixel array manufactured by Spectra Physics (Hilger). A graduated scale is overimposed to show the 200 μm pixel size, 400 μm pitch.

size has been taken into account: H8500 Flat Panel, R8520-C12 and R5900-L16, in order to study the imaging performances of the CsI(Tl) array as a function of scintillation light output and spread.

The Hamamatsu H8500 Flat Panel PMT has a very compact size and a metal wrapping [1]. The external size dimensions are $51.7 \times 51.7 \times 15.4 \text{ mm}^3$, the photocathode is bialkali, with 1.8 mm glass window, and 12 stages of metal channel dynode have been used as electron multiplier. The overall PMT active area of 49.7 squared millimeter, corresponds to an anode area consisting of 8×8 matrix in which each individual anode has a 6 mm side. Anode gain variation results as 48:100.

A 'multi-anode' read out technique was utilized for the Flat Panel Camera, where the charge on each anode is individually read out and digitized. The READ system, was developed at Southampton University; it is capable of reading anode values, calculating the event position at rates in excess of 1000 events per second. The READ system consists of four HX2 16-channel integrating amplifiers with data storage and multiplexed outputs. The serial output from the HX2 board is subsequently read by a 1.5 MHz National Instruments DAQ 6110E Analogue to Digital Converter (ADC) mounted in host PC [2]. The subsequent position determination was performed by applying the centroid method on the total distribution of the charge on the anodic plate.

To evaluate the imager performances by using a smaller PSPMT anode pitch, further experiments involving the Hamamatsu R8520-C12 PSPMT were done [3].

This PMT, as well as the previous models R5900-C12 and R7600-C12, is a compact metal channel dynode PSPMT [3]. It has bialkali photocathode spectral response, and $22 \times 22 \text{ mm}^2$ of area. The first multiplication stage includes a grid which focuses photoelectrons into a $18 \times 18 \text{ mm}^2$ reduced area. Nine metal channel dynode charge multiplication stages produce a typical gain of 10^6 . Twelve cross plate anodes, located on two planes apart (6Y and 6X with a mean size of 3.5 mm), collect the final charge profiles along each axis [4], [5].

The R8520-C12 charge-readout has been performed in a single-photon modality, using single-anode charge readout

electronics. Each anode signal was conditioned by a low-noise charge preamplifier and a shaping amplifier using a 2 μs time-constant. The event-trigger signal was obtained by summing all anode signals. Three National Instruments PCI-6110E computer boards were used for data acquisition. [6].

The data acquisition software was developed using LabWindows C++ (by National Instruments). This software acquires the 12-channel single-event sample and saves the data in a RAM buffer.

Off-line software reconstructs the image filtering valid events by appropriate algorithms (energy window, pulse pile-up, etc.) and calculates the centroid coordinates as:

$$X = \frac{\sum_1^6 w_i q_{Xi}}{\sum_1^6 q_{Xi}}$$

$$Y = \frac{\sum_1^6 w_i q_{Yi}}{\sum_1^6 q_{Yi}}$$

where: w_i is the charge-weight factor assumed linearly proportional to the anode position, and q_{Xi} , q_{Yi} are the digitized charge values along X and Y anodes respectively.

A mono-dimensional PSPMT R5900U-00-L16, with a small anode width, has also been utilized, for a better light sampling. PMT overall dimensions are $26 \times 26 \times 24 \text{ mm}^3$ and the charge multiplication is obtained by a 10-stage metal channel dynode structure [7]. The borosilicate glass window is 1.3 mm thick and the photoelectrons cloud emitted by the bialkali cathode is focused by a grid located before the first dynode. The output charge is collected by 16 parallel anode stripes $0.8 \times 16.0 \text{ mm}^2$, 1 mm pitch. The gain is about 2×10^6 at -800 V . The intrinsic PMT small charge spread produces an intrinsic spatial resolution less than 0.6 mm FWHM for a single photoelectron emission from the photocathode, corresponding to about 0.6 mm FWHM charge spreading [8].

We have utilized the same 'multi-wire' readout electronics and acquisition system of the Flat Panel Camera.

To better evaluate the effect of the different sampling and to enhance the pixel identification, we have performed a few measurements enlarging the light output spread with 1 mm light guide between the scintillator and the PSPMT. The characterization of all imagers was performed by a Co^{57} free and collimated point source, with an output aperture ranging between 0.4 mm and 7 mm. The measurements with the free source was performed setting the detector-source distance at 2 m (flood field irradiation) while the point source, placed at contact with the detector surface, was utilized for crystals scanning, to investigate spatial resolution and position response. In addition, we used a $^{99\text{m}}\text{Tc}$ line source, obtained by shielding a $^{99\text{m}}\text{Tc}$ source with a Pb slab with a 0.2 mm lead slit aperture.

In conclusion, a Monte Carlo simulation has been performed to evaluate possible cross-over effects between crystal pixels generated by the radiation transport. The Monte Carlo code was EGSnrc, latest version,. The simulation includes all the physical processes available with EGS, as Compton and Rayleigh scattering, photoelectric absorption with emission of fluorescence photons or Auger electrons. The lower cut-off energy is fixed to 5 keV for photons and the electron transport was considered. We simulated a 122 keV a parallel beam impinging on the total

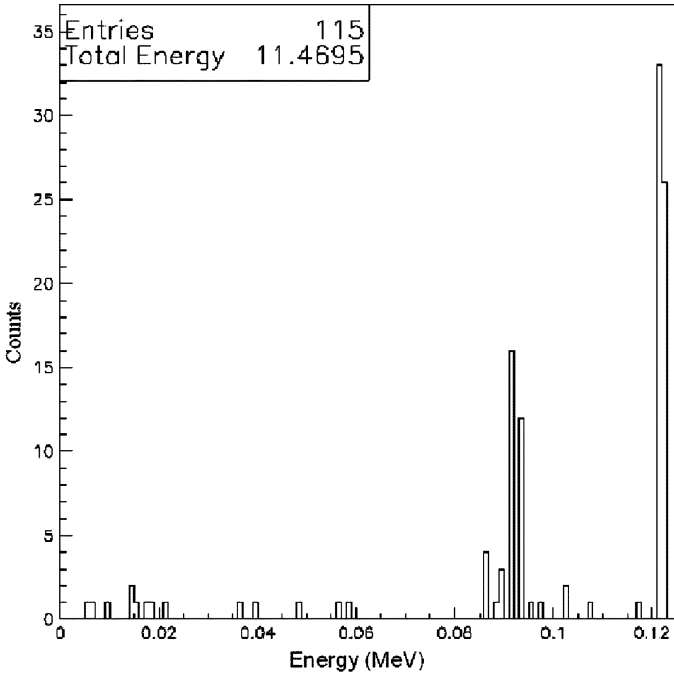


Fig. 2. The simulated energy deposited in one crystal pixel when the total surface of the scintillation array was irradiated at 122 keV by a parallel beam (5 M events). We report the events number (entries) and the total energy deposited in the selected pixel crystal.

area of the scintillator (5 M events) and we studied the number of the events and the energy deposited in each pixel crystal.

III. RESULTS

Fig. 2 shows the simulated pulse height distribution of one pixel crystal when the total surface of the scintillation array was irradiated with a 122 keV by parallel beam. We report also the events number (entries) and the total energy deposited in one selected pixel crystal. As it is clearly visible energy transport is mainly dominated by the escape of X-rays produced by Cs (31.6 keV average K X-ray energy) and I (33.17 keV K-edge) with fluorescence yield of 0.79. The small crystal is able to re-absorb more than 60% of X-rays, limiting the escape peak events at about 50% of the full energy peak. Energy losses due to electron escape are limited to about 15% of total events.

Previously, an estimation of the light spread of the scintillation array was performed by theoretical evaluations and simulations of the light distribution out-coming from the crystal pixel. The following values resulted: 0.8 mm FWHM/1.7 mm FWTM for a 0.8 mm light guide (like a C12 glass window) and 1.8 mm FWHM/3.7 mm FWTM for a 1.8 mm light guide (like a Flat Panel glass window) [9], [10].

We compared these preliminary results with ones obtained coupling the CsI(Tl) micro-pixel array to the three different PSPMT: C12- L16 and Flat Panel. Charge distributions, due to a single scintillation event, collected by the anodes plate of every PSPMT's are shown in Fig. 3. In order to evaluate the effect on light distribution shape of the thickness of glass window, we introduced an additional 1 mm light guide. The analysis of

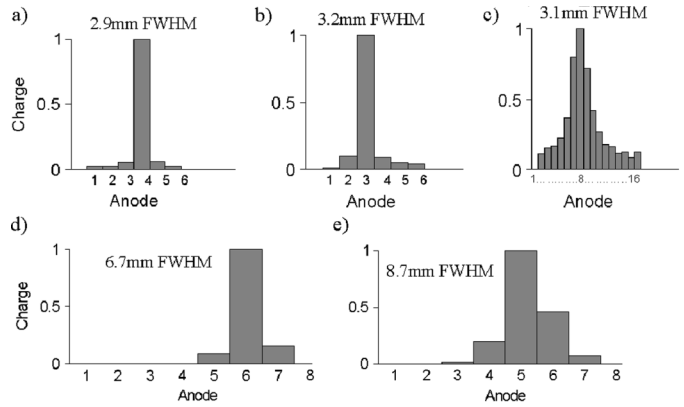


Fig. 3. Charge distribution collected by the anodes plate in different configuration PSPMT/light guide: (a) R8520-C12 PSPMT without light guide; (b) R8520-C12 PSPMT with 1 mm light guide; (c) R5900-L16 PSPMT without light guide; (d) Flat Panel PMT without light guide; (e) Flat Panel PMT with 1 mm light guide.

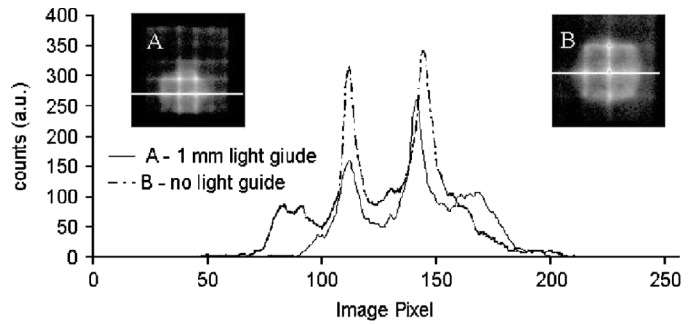


Fig. 4. Image from 7 mm spot irradiation profiles by micro-pixel array coupled to C12 PSPMT. (A) 1 mm light guide; (B) no light guide. The white horizontal line in the image indicates the position where the profile was calculated.

anode charge distributions from the Flat panel [see Fig. 3(d) and (e)] confirmed an enlargement of the charge distribution of more than 8 mm FWHM and more than 10 mm.

The images and the relative profile obtained irradiating with a 7 mm point source the scintillation array coupled to the R8520-C12 PSPMT, with and without light guide, is shown in Fig. 4, where the white horizontal line on the image indicates the position where the relative profile was calculated. The images show an over counting around the center of the anodes, effect highlighted in the profiles, for the anodes principally involved in the measurement. This strong deformation on the position linearity response is probably the result of a non correct light sampling due to the anode size larger than the light spread FWHM [3.5 mm anode size with 2.9 mm, see Fig. 3(a)].

With the addition of 1 mm light guide, in order to flat the light distribution (see image and profile 4A), the position non-linearity is reduced but not eliminated, demonstrating the anode size is still too big to correctly sample such narrow light distributions [3.5 mm respect to 3.2 mm, see Fig. 3(b)].

In order to evaluate the spatial resolution values, we performed a point source irradiation that involved four neighboring anodes, to obtain a right anode sampling of the charge (see Fig. 5). From the image profile it is visible how the peaks are

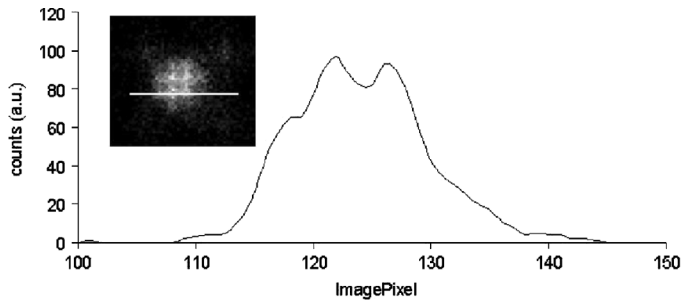


Fig. 5. Image and relative profile of 1 mm spot irradiation by micropixel array coupled to R8520-C12 PSPMT, without light guide. The horizontal line in the image indicates the position where the profile was calculated.

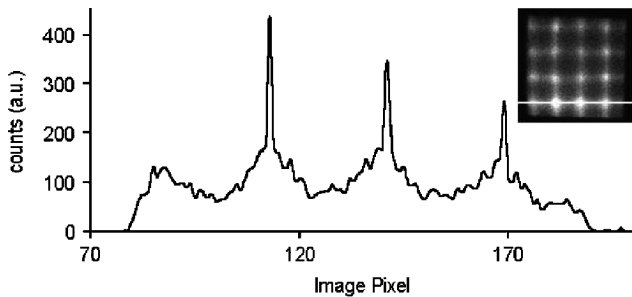


Fig. 6. Flood field profile image by micro-pixel array coupled to Flat Panel PMT. The horizontal line in the image indicates the position where the profile was calculated.

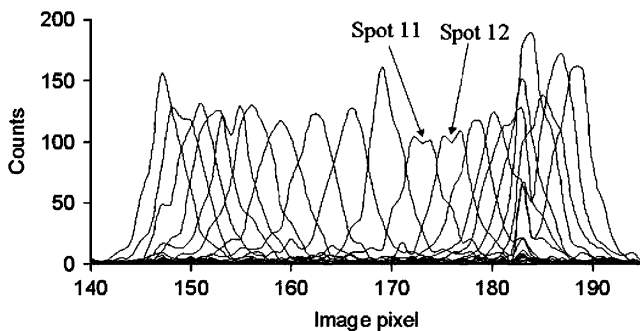


Fig. 7. 0.4 mm spot profile scanning series on the Flat Panel PMT. The arrows indicate the spot 11 and the spot 12 where two anodes are involved in the sampling of the light.

weakly separated and so the spatial resolution value can be assumed a little bit less than the pixel pitch (0.4 mm FWHM).

The flood field irradiation of the scintillation array when coupled to the Flat Panel PMT is shown in Fig. 6, where the overcounting in the center of the anodes is well visible. This profile shows a similar effect obtained by the R8520-C12 PSPMT but the image seems to be more homogeneous.

Finally the detector was irradiated by a 0.4 mm Co^{57} point source and scanned at the same step. In Fig. 7 the image profiles of the scanning series are shown, with the arrows indicating the position where two anodes were involved. The figure shows good response homogeneity of the PMT anodes.

Furthermore a two step scanning was performed by a 0.2 mm ^{99m}Tc slit irradiation. In Fig. 8, the profile of the slit irradiation is shown, and the distance between the slits is indicated to stress the good spatial resolution of the detector.

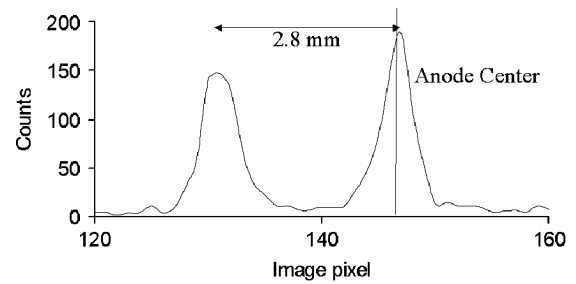


Fig. 8. 0.2 mm slit by Tc^{99m} irradiations on a Flat Panel PMT.

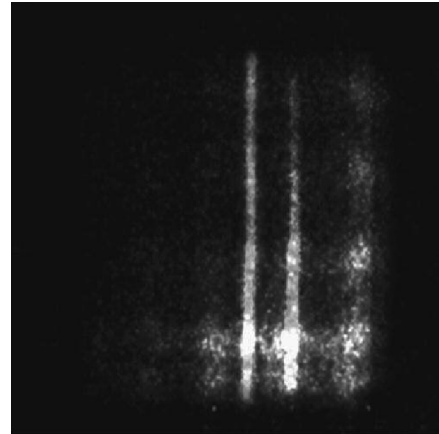


Fig. 9. A couple of 0.2 mm slit ^{99m}Tc irradiations, 2.8 mm apart on the Flat Panel PMT.

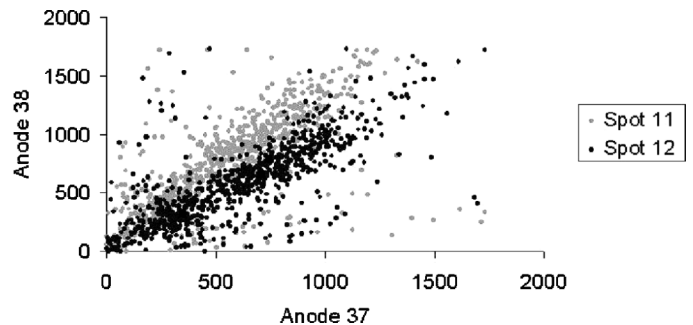


Fig. 10. Charge ratio between 38 and 37 anodes for each event.

Fig. 9 shows the image obtained with the two line irradiations 2.8 mm apart. A spatial resolution of about 0.6 mm resulted.

In Fig. 10 we present the charge collected by two anodes involved in two point source irradiations: the charge ratio between the two anodes varied when passing from a spot to another one, demonstrating the detector ability in position sensing (see spot 11 and 12 in Fig. 7).

In Fig. 11, we report the image profiles obtained by a 0.4 mm collimated irradiation and a 0.2 mm collimated slit irradiation, with and without 1 mm light guide for the Flat Panel PSPMT. The spatial resolution values indicated in figure ranged between 0.6 and 0.7 mm, demonstrating a spatial resolution limit for this setup. A worse spatial resolution value results by the additional 1 mm light guide. Such results were further confirmed by a measure of the average MTF obtained by a spot irradiation (PSF) of CsI(Tl) crystal array (see Fig. 12).

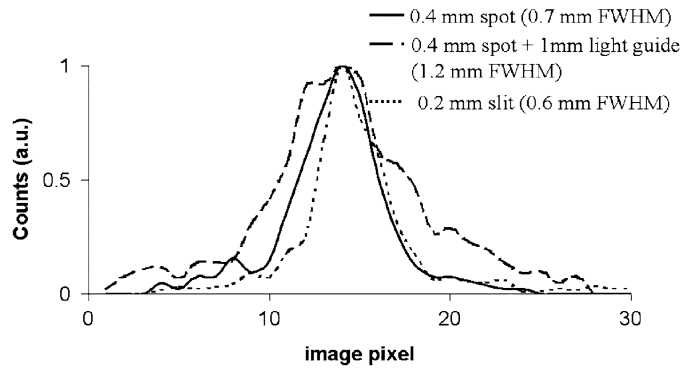


Fig. 11. Flat Panel profile image by a 0.4 mm collimated irradiation and a 0.2 mm collimated slit irradiation (with and no 1 mm light guide).

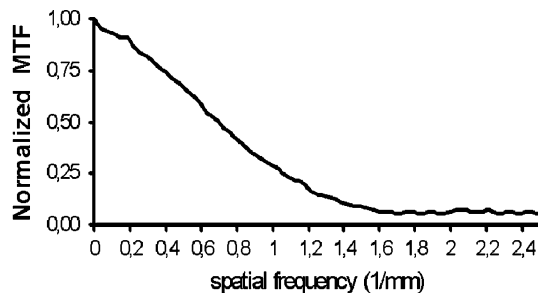


Fig. 12. MTF shape obtained as Fourier transform of spot image (PSF).

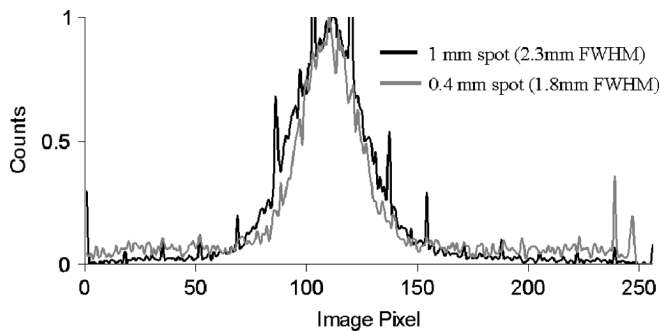


Fig. 13. 0.4 mm and 1 mm spot irradiation on R5900-L16 PMT.

Fitting with a Gaussian profile, in the frequency domain we obtain:

$$\text{FWHM}(k) = 2,35/(2\sigma\pi) = 1,58 \text{ mm}^{-1}$$

that corresponds to:

$$\text{FWHM}(x) = 2,35 \cdot \sigma = 2,352/(2\pi \cdot \text{FWHM}(k)) \sim 0,55 \text{ mm}.$$

This value represents the intrinsic spatial resolution limit for an energy resolution of 50% at 122 keV. The intrinsic spatial resolution values worse than a pixel size, can be explained by the poor crystal light output and by a too big anode size for such a narrow light distribution.

In addition the R5900-L16 PMT was used to reduce the anodic step for charge distribution sampling. The camera was scanned by 0.4 mm and 1 mm spot, with a scanning step of 0.375 mm. The results are shown in Fig. 13.

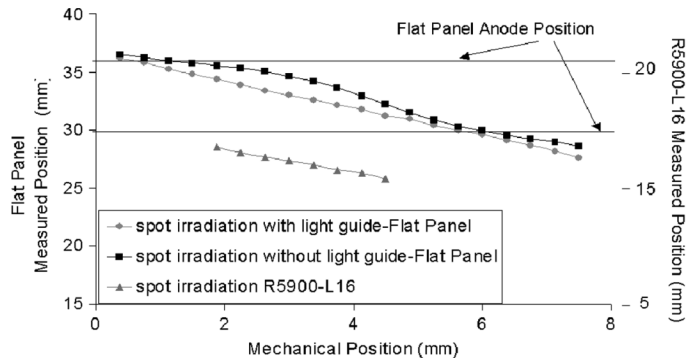


Fig. 14. Flat Panel and R5900-L16 linearity for 0.4 mm spot irradiation series.

The smaller anode size, in reference to the Flat Panel, implies a better linearity as shown in Fig. 14, where the non linearity of the Flat Panel without an additional light guide is clearly visible.

The mean charge distribution obtained by R5900-L16 is shown in Fig. 4(c) confirming previous FWHM values obtained by R8520-C12 (Fig. 4(a)–(b)). In contrast to the other two PSPMTs, R5900-L16 carries out the worst spatial resolution values as a shown in Fig. 13. This phenomena can be explained by the presence of the tails on the charge distribution, that increase when the anode size is reduced, as it can be seen by a comparison with R8520-C12.

In our opinion, when the light output from the scintillator is low, the reduction of anodic size strongly reduces the anodic signal and increases the contribution of the noise on the charge distribution. This effect is magnified by the anodic strip structure (C8 and C12 PSPMT). It is confirmed by the spatial resolution values resulting non-sensitive to irradiation spot size, demonstrating how the measurements were mainly affected by PMT noise. The preliminary measurements show a better performance of the Flat panel PMT, that carries out an intrinsic spatial resolution limit of about 0.6 mm FWHM.

We are not able to fully explain the mayor result by the Flat Panel PMT, as well the charge distribution measured about two time larger then the one obtained by the other PSPMTs. The only possible explanation could be found in the structure of electron focusing grid with the same size of the anode but not aligned with it; in fact, that could produce a broadening of the charge spread when the light spot is centered on a single anode.

IV. CONCLUSIONS

Taking into account a loosing of light output more than five times lower than the regular CsI(Tl) array configuration, excellent spatial resolution values resulted by coupling micro-pixel array to PSPMT. The Flat Panel PMT shows a superior response even though a thicker photocathode glass window and a larger anode size with respect to the previous generation PSPMTs. The next generation Flat Panel PMT with 3 mm anode size and a reduction of photocathode glass window thickness to 1.5 mm can foresee very good performances for sub-millimetric spatial resolution imaging and can justify efforts in producing scintillation array with hundred micron pixel size.

REFERENCES

- [1] *Hamamatsu Photonics K.K.*, R8500, Electron Tube Center, 2002, Flat Panel Data Sheet.
- [2] R. Pani, R. Pellegrini, M. N. Cinti, C. Trotta, G. Trotta, R. Scafè, L. D'Addio, G. Iurlaro, L. Montani, P. Bennati, S. Ridolfi, F. Cusanno, and F. Garibaldi, "Factors affecting flat panel PMT calibration for gamma ray imaging," in *Proc. IEEE Nuclear Science Symp. Conf. Rec.*, Norfolk, VA, Nov. 2002, vol. 10–16, no. 2, pp. 671–675.
- [3] *Hamamatsu Photonics K.K.*, H8520-00-C12, Electron Tube Center, 2000, B-21 Data Sheet.
- [4] M. Watanabe, T. Omura, H. Kyushima, Y. Hasegawa, and T. Yamashita, "A compact position-sensitive detector for PET," *IEEE Trans. Nucl. Sci.*, vol. 42, no. 4, pp. 1090–1094, Aug. 1995.
- [5] Y. Yoshizawa and J. Takeuchi, "The latest vacuum photodetector," in *Nucl. Instrum. Methods Phys. Res. A*, 1997, vol. A387, pp. 33–37.
- [6] *National Instruments Corporation*, PCI-6110E/6111E Multifunction I/O Boards for PCI Bus Computers, 1998, User Manual.
- [7] *Hamamatsu Photonics K.K.*, R5900-00-L16, Electron Tube Center, 2003, Data Sheet.
- [8] D. Grigoriev, O. Johnson, W. Worstell, and V. Zavarzin, "Characterization of a new multianode PMT for low-level optical fiber readout," *IEEE Trans. Nucl. Sci.*, vol. 44, no. 3, pp. 990–993, Jun. 1997.
- [9] R. Scafè, R. Pellegrini, A. Soluri, N. Burgio, G. Trotta, A. Tati, M. N. Cinti, G. De Vincentis, and R. Pani, "Light output spatial distributions of CsI(Tl) scintillation arrays for gamma-rays imaging," *Nucl. Instrum. Methods Phys. Res. A*, vol. A497, pp. 249–254, 2003.
- [10] R. Scafè, R. Pellegrini, S. Soluri, A. Tati, M. N. Cinti, F. Cusanno, G. Trotta, R. Pani, and F. Garibaldi, "A study of intrinsic crystal-pixel light-output spread for discrete scintillation gamma-rays imagers modeling," in *Proc. IEEE Nuclear Science Symp. and Medical Imaging Conf. Rec.*, Norfolk, VA, 2002, pp. 1652–1655.